Supplementary Information : Exciton spectroscopy and unidirectional transport in $MoSe_2$-WSe_2 lateral heterostructures encapsulated in hexagonal boron nitride

Dorian Beret[1,+], Ioannis Paradisanos[1,+], Hassan Lamsaadi[2,+], Ziyang Gan[3,+], Emad Najafidehaghani[3], Antony George[3,4], Tibor Lehnert[5‡], Johannes Biskupek[5], Ute Kaiser[5], Shivangi Shree[6], Ana Estrada-Real[1,7], Delphine Lagarde[1], Xavier Marie[1], Pierre Renucci[1], Kenji Watanabe[8], Takashi Taniguchi[9], Sebastian Weber[2], Vincent Paillard[2], Laurent Lombez[1],* Jean-Marie Poumirol[2],† Andrey Turchanin[3,4],‡ and Bernhard Urbaszek[1,7§]

[1] *Université de Toulouse, INSA-CNRS-UPS, LPCNO, 135 Avenue Rangueil, 31077 Toulouse, France*

[2] *CEMES-CNRS, Université de Toulouse, Toulouse, France*

[3] *Friedrich Schiller University Jena, Institute of Physical Chemistry, 07743 Jena, Germany*

[4] *Abbe Centre of Photonics, 07745 Jena, Germany*

[5] *Ulm University, Central Facility of Electron Microscopy, D-89081 Ulm, Germany*

[6] *Department of Physics, University of Washington, Seattle, WA, USA.*

[7] *Institute of Condensed Matter Physics, Technische Universität Darmstadt, Germany*

[8] *Research Center for Functional Materials, National Institute for Materials Science, 1-1 Namiki, Tsukuba 305-0044, Japan and*

[9] *International Center for Materials Nanoarchitectonics, National Institute for Materials Science, 1-1 Namiki, Tsukuba 305-0044, Japan*

CONTENTS

* laurent.lombez@cnrs.fr

† jean-marie.poumirol@cemes.fr

‡ andrey.turchanin@uni-jena.de

§ bernhard.urbaszek@pkm.tu-darmstadt.de

Supplementary Note 1. Optical microscope image and linescan description

An optical microscope image of the $MoSe_2/WSe_2$ lateral heterostructure (LH) and a schematic representation of the linescan process used in the optical spectroscopy experiments are shown in Fig. 1a,b. We use water-assisted deterministic transfer to pick up as-grown, chemical vapor deposition (CVD) LHs using polydimethylsiloxane (PDMS) and deterministically transfer and encapsulate them in hBN [1, 2]. The optical contrast between $MoSe_2$ and WSe_2 is different, allowing the direct visualization of the heterojunctions, shown with white dashed lines in Fig. 1a. In Fig. 1b we show a schematic representation of the process for the Raman, PL and Reflectivity linescans (Figure1 in the main text). We position the excitation laser ($\lambda = 633$ nm, diffraction-limited spot diameter of 1 μm) on the area of WSe_2 and we use piezo-controlled nanopositioners to move the sample with steps of ≈ 150 nm. After each step, a single -Raman, photoluminescence, reflectivity- spectrum is collected and finally all spectra are plotted as contour representations in Figure1 of the main text.

Supplementary Note 2. Optical spectroscopy

Raman, PL and differential white light reflectivity spectra are collected at T=5 K in a closed-loop liquid helium (LHe) system. Fig. 2a,b,c shows individual Raman, PL and reflectivity spectra of $MoSe_2$ (bottom), junction (middle) and WSe_2 (top), after transfer and encapsulation in hBN. For the Raman and PL experiments we use a 633 nm HeNe laser as an excitation source with a spot size diameter of ≈ 1 μm and 6 μW power. In reflectivity we use a tungsten-halogen white light source with a power of a few nW to collect the intensity reflection coefficient of the sample with the monolayer (R_{ML}) and the reflection coefficient of the substrate (R_S) so that $\Delta R = (R_{ML} - R_S)/R_S$. The spectral shape and

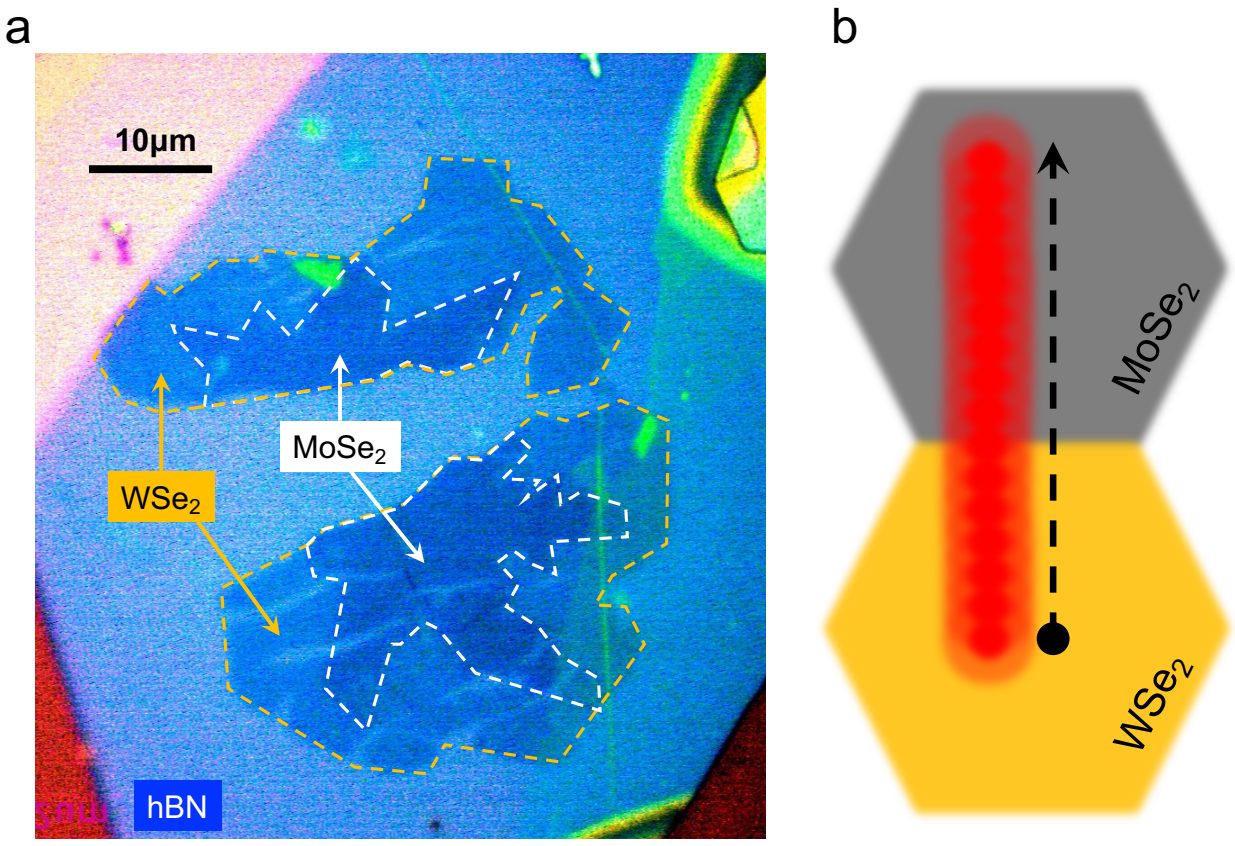

Supplementary Figure 1. (a) Optical image of the hBN-encapsulated LH. Orange and white dashed lines indicate the boundaries of WSe_2 and $MoSe_2$, respectively. (b) Schematic representation of the Raman, PL and Reflectivity linescan process across the heterojunction of $MoSe_2/WSe_2$ LH. The laser is initially positioned on WSe_2 and a series of sequential steps (step size $\approx$ 150 nm) follows with a single signal acquisition after each step.

amplitude of the differential reflectivity signal also depends on thin-film interference effects related to the thickness of top, bottom hBN and SiO_2 layers [3]

The main Raman peaks of $MoSe_2$ (Fig. 2a) include the $A_1'(\Gamma)$ phonon at 241 cm^{-1} and the $E'(\Gamma)$ at 291 cm^{-1} [4], while a strong peak at 458 cm^{-1} has been associated two other peaks to form triplets, see supplementary material of [5]. A strong peak at 531 cm^{-1} was recently assigned to multi-phonon processes either associated with both K and M point phonons or combinations of Γ point phonons [5]. The observation of this phonon is a signature of resonant excitation with an excited exciton state. WSe_2 phonons are spectrally different compared to $MoSe_2$. The degenerate $A_1'(\Gamma)/E'(\Gamma)$ phonons are located at 250 cm^{-1} and, similar to $MoSe_2$, a strong and recently discovered peak at 495 cm^{-1} is also observed here

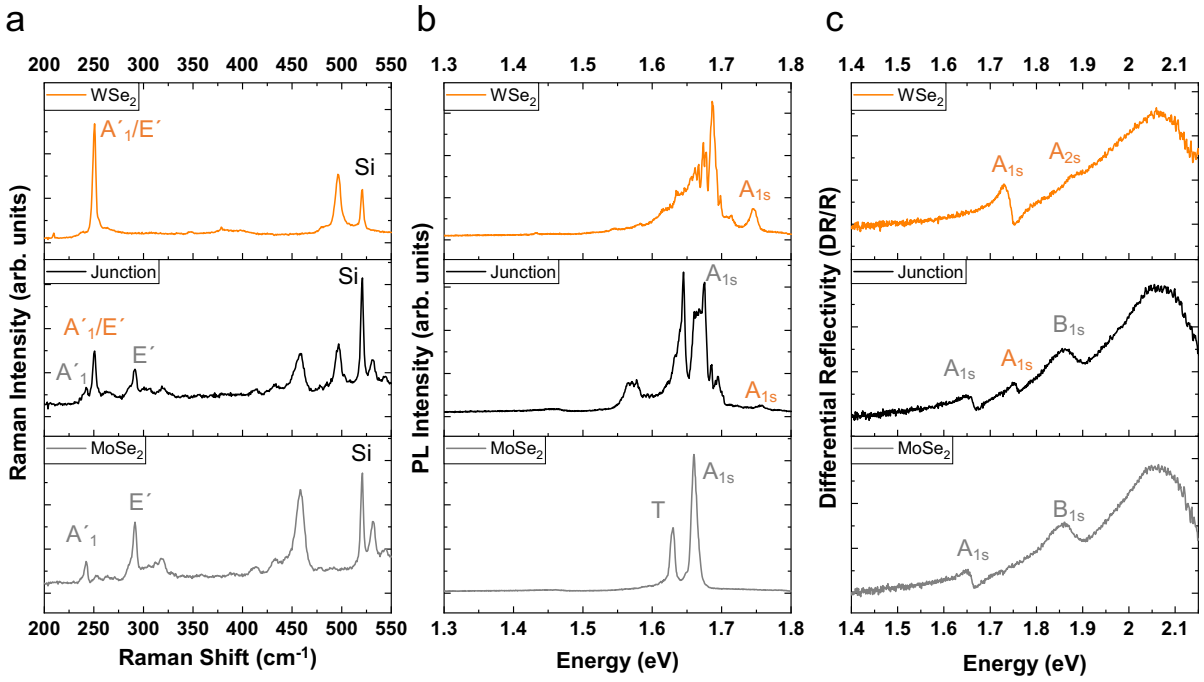

Supplementary Figure 2. (a) Raman, (b) photoluminescence and (c) reflectivity spectra of $MoSe_2$ (bottom), on the junction (middle) and WSe_2 (top).

and attributed to multi-phonon processes at K and M points or combination of Γ point phonons [5]. As expected, when the laser spot is on the junction, Raman spectra display a superposition of the individual spectral signatures. We did not identify any measurable shift or broadening of the Raman peaks when we scanned across the junction. PL spectra of $MoSe_2$ and WSe_2 monolayers exhibit pronounced peaks (Fig. 2b), associated with neutral neutral (X^0) and charged (X^T) excitons. Additional peaks appearing at lower energies, especially in WSe_2 and at the junction, possibly due to an ensemble of localized emission from defects. Further experiments are necessary to examine any possibility of the formation of interlayer excitons. Strong excitonic resonances appear in reflectivity for both materials with negligible Stokes shift between emission and absorption of the A1s exciton state (see Fig. 2c). Clear signatures of B1s states are also observed in both materials while for WSe_2 the appearance of the A2s excited state further supports the good quality of the CVD-grown monolayers. Similar to Raman and PL spectroscopy, on the junction we observe a superposition of the available states from both materials.

Supplementary Note 3. Diffusion experiment and model

For the investigation of lateral transport, we used an experimental procedure very similar to the one described in Supplementary Note 1. The excitation is based on a HeNe laser with an excitation spot size of about 0.7μm and an excitation power of 5μW. The PL images are recorded by a Hamamatsu Fusion-BT CMOS camera. The PL profiles are plotted in polar coordinates. To do so, we integrate over all the polar angles [0;2π], the data are therefore $I_{PL}(r)$ where r is the radius from the maximum PL intensity.

To model the scanning part over the junction (see Fig.4 in the main text), we numerically solved the classical diffusion equation with the use of the Matlab toolbox *pdetool* (partial differential equation toolbox).

Supplementary Note 4. Electron microscopy

For STEM investigation, the samples were transferred to Quantifoil^{tm} grids using PMMA assisted transfer protocol. The High-angle annular dark-field scanning transmission electron microscopy (HAADF-STEM) image was acquired with a Thermofisher Talos 200X microscope operated at 200 kV.

---

[1] Jia, H. *et al.* Large-scale arrays of single-and few-layer mos 2 nanomechanical resonators. *Nanoscale* **8**, 10677–10685 (2016).

[2] Paradisanos, I. *et al.* Controlling interlayer excitons in mos 2 layers grown by chemical vapor deposition. *Nature communications* **11**, 1–7 (2020).

[3] Robert, C. *et al.* Optical spectroscopy of excited exciton states in mos_2 monolayers in van der waals heterostructures. *Phys. Rev. Materials* **2**, 011001 (2018).

[4] Soubelet, P., Bruchhausen, A. E., Fainstein, A., Nogajewski, K. & Faugeras, C. Resonance effects in the raman scattering of monolayer and few-layer mose 2. *Physical Review B* **93**, 155407 (2016).

[5] McDonnell, L. P., Viner, J. J., Rivera, P., Xu, X. & Smith, D. C. Observation of intravalley phonon scattering of 2s excitons in mose2 and wse2 monolayers. *2D Materials* **7**, 045008 (2020).

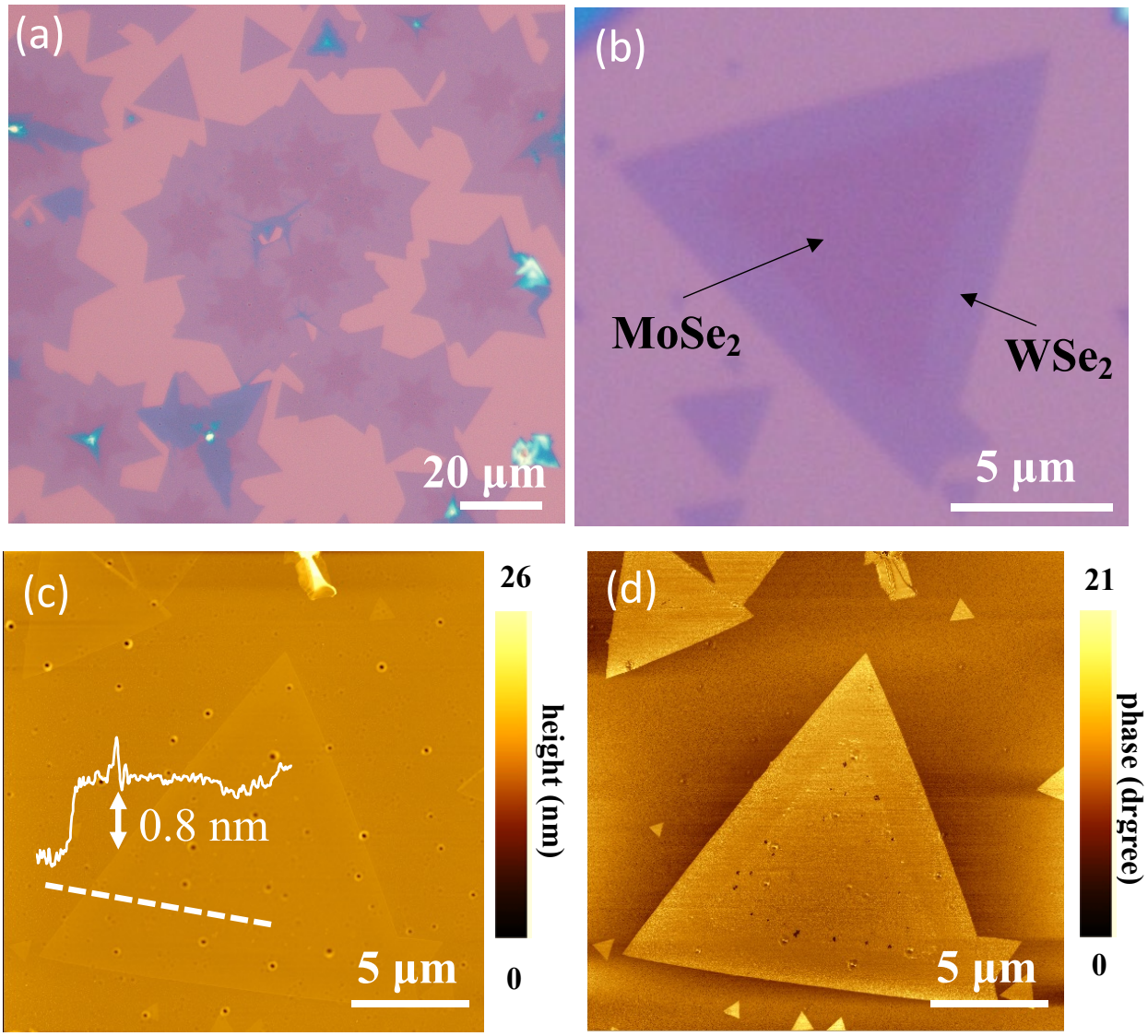

Supplementary Figure 3. **Characterization of lateral heterostructures** (a,b) Optical microscopy image of as grown $MoSe_2$-WSe_2 LHs (c,d) AFM height and phase image of as grown LHs. The height profile in the inset of (c) shows monolayer thickness of 0.8 nm.

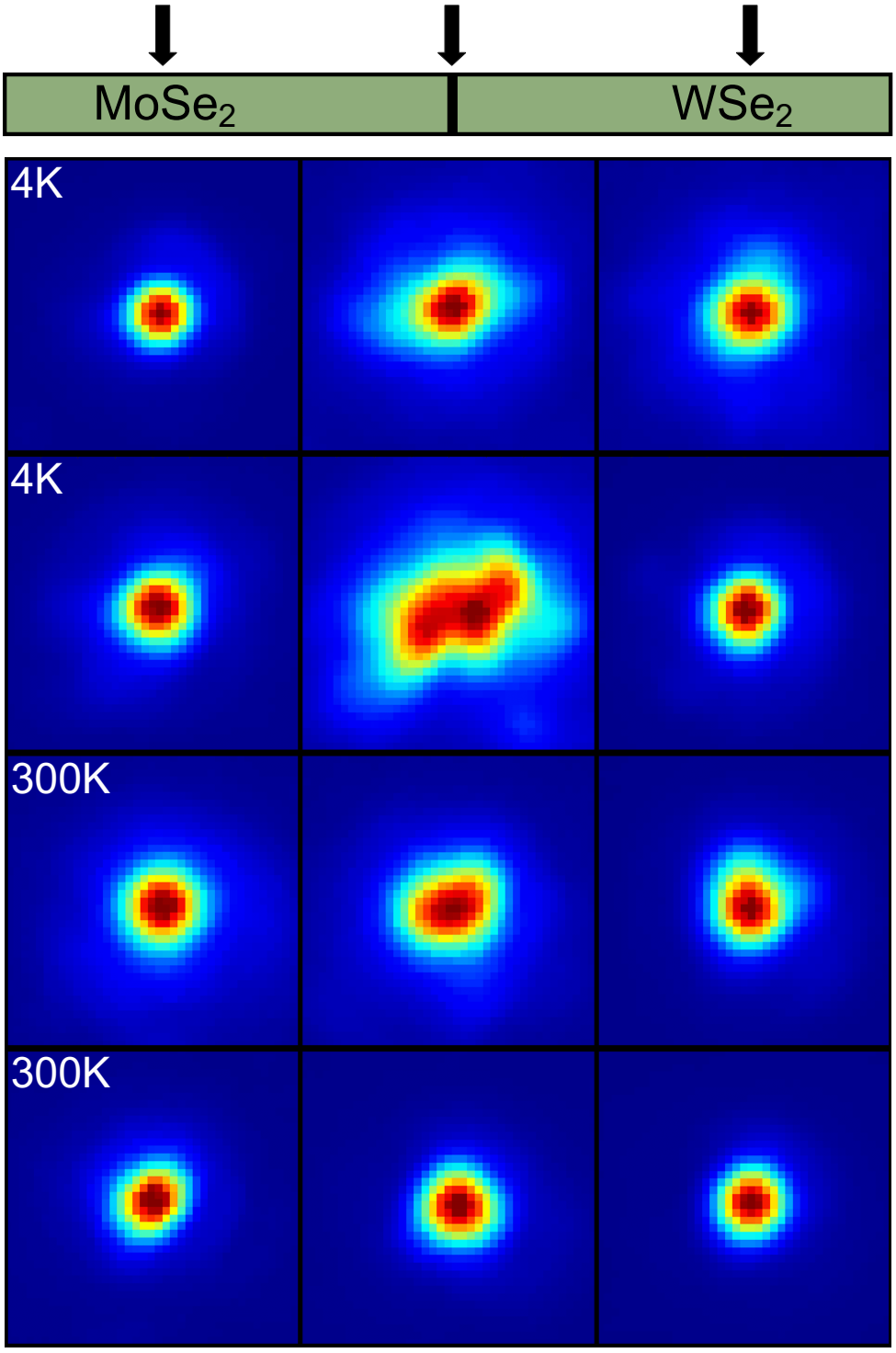

Supplementary Figure 4. **More examples of PL imaging** We show more examples of typical PL emission spots in $MoSe_2$ (left), on the junction between the two materials (middle), and in WSe_2 (right) for two different sample temperatures as marked on the panels for each line.